





Article

Macrocyclic Ionic Liquids with Amino Acid Residues: Synthesis and Influence of Thiacalix[4]arene Conformation on Thermal Stability

Olga Terenteva¹, Azamat Bismukhametov¹ , Alexander Gerasimov¹ , Pavel Padnya^{1,*} 
and Ivan Stoikov^{1,2,*} 

¹ A.M. Butlerov Chemistry Institute, Kazan Federal University, 18 Kremlevskaya Street, Kazan 420008, Russia

² Federal Center for Toxicological, Radiation and Biological Safety, 2 Nauchny Gorodok Street, Kazan 420075, Russia

* Correspondence: padnya.ksu@gmail.com (P.P.); ivan.stoikov@mail.ru (I.S.); Tel.: +7-843-233-7241 (I.S.)

Abstract: Novel thiacalix[4]arene based ammonium ionic liquids (ILs) containing amino acid residues (glycine and *L*-phenylalanine) in *cone*, *partial cone*, and *1,3-alternate* conformations were synthesized by alkylation of macrocyclic tertiary amines with *N*-bromoacetyl-amino acids ethyl ester followed by replacing bromide anions with bis(trifluoromethylsulfonyl)imide ions. The melting temperature of the obtained ILs was found in the range of 50–75 °C. The effect of macrocyclic core conformation on the synthesized ILs' melting points was shown, i.e., the ILs in *partial cone* conformation have the lowest melting points. Thermal stability of the obtained macrocyclic ILs was determined via thermogravimetry and differential scanning calorimetry. The onset of decomposition of the synthesized compounds was established at 305–327 °C. The compounds with *L*-phenylalanine residues are less thermally stable by 3–19 °C than the same glycine-containing derivatives.

Keywords: thiacalix[4]arenes; ionic liquids; amino acid; synthesis; thermal stability; melting point



Citation: Terenteva, O.; Bismukhametov, A.; Gerasimov, A.; Padnya, P.; Stoikov, I. Macrocyclic Ionic Liquids with Amino Acid Residues: Synthesis and Influence of Thiacalix[4]arene Conformation on Thermal Stability. *Molecules* **2022**, *27*, 8006. <https://doi.org/10.3390/molecules27228006>

Academic Editors: Slavica Ražić, Aleksandra Cvetanović Kljakić and Enrico Bodo

Received: 1 November 2022

Accepted: 16 November 2022

Published: 18 November 2022

Publisher's Note: MDPI stays neutral with regard to jurisdictional claims in published maps and institutional affiliations.



Copyright: © 2022 by the authors. Licensee MDPI, Basel, Switzerland. This article is an open access article distributed under the terms and conditions of the Creative Commons Attribution (CC BY) license (<https://creativecommons.org/licenses/by/4.0/>).

1. Introduction

Ionic liquids (ILs) have been attracting the attention of researchers in the last two decades. Their unique properties, e.g., low vapor pressure, low toxicity, recyclability, high solvating ability, polarity, thermal and electrochemical stability and electrical conductivity can be explained by the structure [1–16]. ILs consist of bulky organic cations with low symmetry and inorganic or organic anions [17]. The physicochemical properties of ILs can also be affected by varying the cations and anions [18].

Despite the fact that the first examples of ILs are derivatives of ammonium salts, this class of compounds has not been fully investigated. Ammonium ILs were used for metal ions extraction, functional materials creation, as a reaction medium, battery electrolytes, components of pharmaceutical agents [19–23]. However, low biocompatibility and complexation selectivity limit the practical application of these compounds. A possible solution of this problem is the modification of ILs with various functional groups, e.g., amide, hydroxyl, carboxyl, amino acid fragments etc. ILs with amino acid fragments also increase the stability of biomolecules such as enzymes and DNA [24–29]. Prior works showed the rise of thermal stability and effect of such ILs on proteins activity and stability, their package changing and aggregation inhibition [30–33].

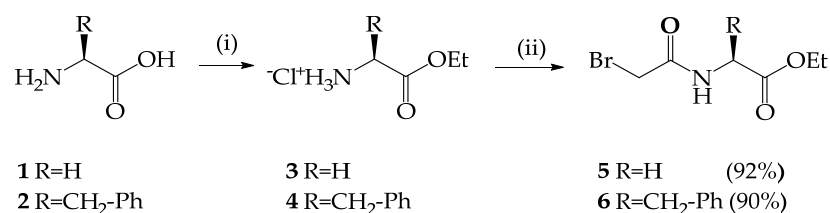
One of the actively developing classes of ILs are macrocyclic and polyionic liquids containing several cationic fragments [34–36]. The design of ILs based on supramolecular platforms, e.g., crown ethers [37], pillararenes [38–40], and (thia)calixarenes [41–47], was described. At this moment, the creation of such structures is a non-trivial synthetic problem. Only a few examples of their successful synthesis are known [48,49]. Our scientific group has shown that the introduction of quaternary ammonium, ester and amino acid fragments

leads to obtain macrocyclic ILs in *cone* and *1,3-alternate* conformations [50]. There are no literature examples of the synthesis and properties study of macrocyclic ILs based on *partial cone* stereoisomer. The structure of *partial cone* is less symmetrical than *cone* and *1,3-alternate*, that can hypothetically decrease the melting point of such compounds. The introduction of different amino acid residues affects the thermal stability and melting point, which are important characteristics of ILs. In this work, *p*-*tert*-butylthiacalix[4]arenes tetrasubstituted at the lower rim with quaternary ammonium groups and amino acid fragments (glycine and *L*-phenylalanine) in *cone*, *partial cone*, and *1,3-alternate* conformations were synthesized for the first time. The influence of the conformation of macrocyclic core and the nature of the amino acid substituent on their thermal stability was investigated.

2. Results and Discussion

2.1. Synthesis of *p*-*tert*-butylthiacalix[4]arenes Containing Quaternary Ammonium Groups and Fragments of Glycine and *L*-phenylalanine

Previously, our scientific group developed an approach to the synthesis of macrocyclic ILs [50]. It consisted in the alkylation of *p*-*tert*-butylthiacalix[4]arene-based tertiary amines, followed by the replacement of bromide anions. Initially, we synthesized highly reactive alkylating agents containing amino acid residues. Glycine **1** and *L*-phenylalanine **2** were selected to evaluate the effect of planar π -aromatic ring systems on physical properties, e.g., melting point and thermal stability. The target compounds were obtained in two steps (Scheme 1). The first step was the synthesis of the amino acid esters **3** and **4**. The second step was the interaction of the obtained compounds **3** and **4** with bromoacetic acid bromide. *N*-Bromoacetyl-amino acid ethyl esters **5** and **6** were obtained in 92 and 90% yield.

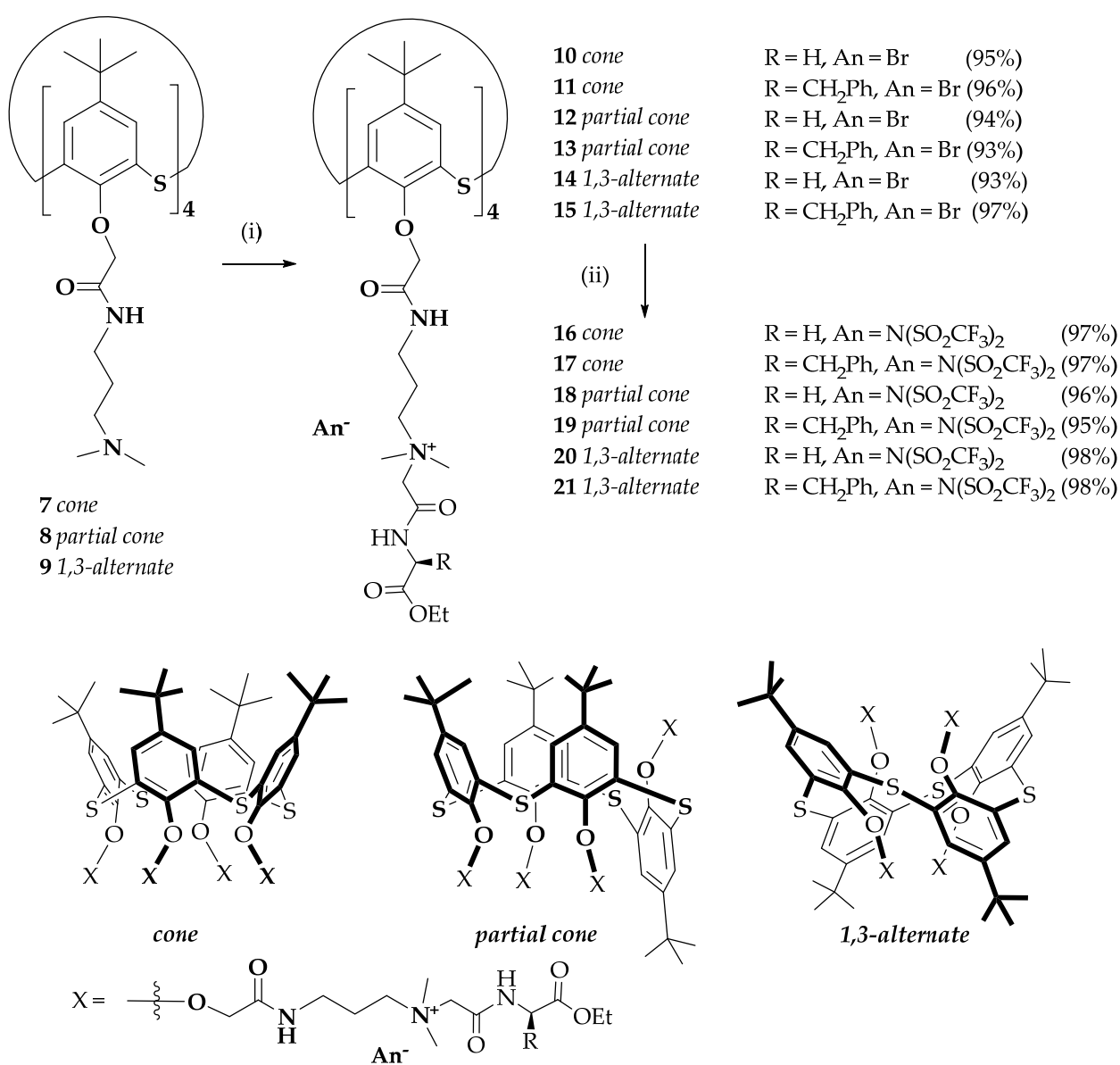


Scheme 1. Reagents and reaction conditions: (i) SOCl_2 , ethanol; (ii) $\text{BrCH}_2\text{C}(\text{O})\text{Br}$, NaHCO_3 , benzene/water.

The next stage of this work was the study of reaction of the obtained alkylating agents **5** and **6** with tetrasubstituted thiacalixarenes **7–9** containing terminal tertiary amino groups in *cone*, *partial cone* and *1,3-alternate* conformations (Scheme 2). Targeted bromides of macrocyclic quaternary ammonium salts **10–15** were obtained in high yields (93–95%). Previously, a significant decrease in the melting point by replacing halide ions with bis(trifluoromethylsulfonyl)imide ions ($\text{N}(\text{SO}_2\text{CF}_3)_2^-$, NTf_2^-) has also been shown [51]. This can be explained by the fact that the increase of anion size decreases symmetry of the molecule. Thus, the compounds **10–15** were reacted with lithium bis(trifluoromethylsulfonyl)imide in water at room temperature. The macrocyclic ILs **16–21** were obtained in yields close to quantitative (Scheme 2).

The structure and the composition of all synthesized compounds were confirmed by ^1H and ^{13}C NMR, IR spectroscopy, mass spectrometry and elemental analysis (Figures S1–S33). The conformation of modified *p*-*tert*-butylthiacalix[4]arene derivatives can be determined by one-dimensional ^1H NMR spectroscopy based on specific proton signals of *tert*-butyl group, aromatic ring, oxymethylene and amide group. Table 1 lists the values of the characteristic chemical shifts of the compounds **10–21**. The protons of oxymethylene and amide groups of the compound **15** (*1,3-alternate*) are located in the shielded zone of neighboring aromatic rings of the macrocycle. These signals in the ^1H NMR spectrum are recorded upfield (4.00 and 8.02 ppm, respectively) of those of the macrocycles **11** in *cone* conformation (4.81 and 8.50 ppm, respectively). The chemical shifts of the aromatic protons depend less on the conformation of the macrocyclic platform, shifting by only 0.20 ppm upfield from *cone* **11** (7.39 ppm) to *1,3-alternate* **15** (7.59 ppm) stereoisomers. This

provides evidence of the shielding effect of neighboring aryl fragments in *cone* stereoisomer on the aryl protons of macrocycle ring. The *tert*-butyl groups proton signals of *cone* **11** were found upfield (1.07 ppm) in contrast to the same signals of *1,3*-*alternate* **15** (1.19 ppm). This effect was related to the spatial location of the *tert*-butyl groups of *1,3*-*alternate* stereoisomer shielded by neighboring fragments of the macrocycle. The proton signals in *partial cone* **13** differ from *cone* and *1,3*-*alternate* due to the asymmetric structure of the macrocycle. The *tert*-butyl groups proton signals of *partial cone* **13** were recorded upfield (1.00, 1.10 and 1.27 ppm) as singlets with 2:1:1 intensity ratio. The oxymethylene proton signals were located in 4.40–4.77 ppm as two singlets and an AB-system. The aromatic ring proton signals are recorded at 7.67, 7.75, 7.01–7.65 ppm as two singlets and an AB-system. The amide group proton signals appeared in 8.31–8.48 ppm as broadened triplets. This effect of AB-systems in the ^1H NMR spectra due to the asymmetry of *partial cone* stereoisomer structure shielded by neighboring aromatic fragments of the macrocycle.



Scheme 2. Reagents and reaction conditions: (i) *N*-bromoacetyl-amino acid ethyl esters **5** or **6**, acetonitrile; and (ii) LiN(SO₂CF₃)₂, water.

Table 1. Chemical shifts (ppm) and spin-spin coupling constants (Hz) in the ^1H NMR spectra of the compounds **10–21** (DMSO- d_6 , 298 K, 400 MHz).

Compounds	Amino Acid Fragments/Anion	^tBu	OCH_2	ArH	$\text{NHCH}_2\text{CH}_2\text{CH}_2\text{N}^+$
10 (<i>cone</i>) *	Gly/ Br^-	1.12	5.03	7.36	8.68
11 (<i>cone</i>)	<i>L</i> -Phe/ Br^-	1.07	4.81	7.39	8.50
12 (<i>partial cone</i>)	Gly/ Br^-	1.00, 1.17, 1.27	4.40 ($^2J_{\text{HH}} = 13.6$ Hz), 4.49, 4.51, 4.80 ($^2J_{\text{HH}} = 13.6$ Hz)	7.67, 7.01 ($^4J_{\text{HH}} = 2.4$ Hz), 7.65 ($^4J_{\text{HH}} = 2.4$ Hz), 7.75	8.36, 8.45, 8.50
13 (<i>partial cone</i>)	<i>L</i> -Phe/ Br^-	1.00, 1.10, 1.27	4.42 ($^2J_{\text{HH}} = 13.5$ Hz), 4.48, 4.51, 4.79 ($^2J_{\text{HH}} = 13.5$ Hz)	7.67, 7.01 ($^4J_{\text{HH}} = 2.4$ Hz), 7.65 ($^4J_{\text{HH}} = 2.4$ Hz), 7.75	8.31, 8.41, 8.48
14 (<i>1,3-alternate</i>) *	Gly/ Br^-	1.20	3.99	7.60	8.04
15 (<i>1,3-alternate</i>)	<i>L</i> -Phe/ Br^-	1.19	4.00	7.59	8.02
16 (<i>cone</i>) *	Gly/ NTf_2^-	1.11	4.89	7.35	8.48
17 (<i>cone</i>)	<i>L</i> -Phe/ NTf_2^-	1.06	4.79	7.38	8.48
18 (<i>partial cone</i>)	Gly/ NTf_2^-	1.00, 1.27, 1.30	4.39 ($^2J_{\text{HH}} = 13.6$ Hz), 4.49, 4.51, 4.78 ($^2J_{\text{HH}} = 13.6$ Hz)	7.67, 7.01 ($^4J_{\text{HH}} = 2.4$ Hz), 7.65 ($^4J_{\text{HH}} = 2.4$ Hz), 7.75	8.31, 8.41, 8.50
19 (<i>partial cone</i>)	<i>L</i> -Phe/ NTf_2^-	1.00, 1.27, 1.28	4.40 ($^2J_{\text{HH}} = 13.5$ Hz), 4.49, 4.52, 4.79 ($^2J_{\text{HH}} = 13.5$ Hz)	7.67, 7.02 ($^4J_{\text{HH}} = 2.4$ Hz), 7.65 ($^4J_{\text{HH}} = 2.4$ Hz), 7.75	8.28, 8.40, 8.48
20 (<i>1,3-alternate</i>) *	Gly/ NTf_2^-	1.20	3.99	7.59	8.03
21 (<i>1,3-alternate</i>)	<i>L</i> -Phe/ NTf_2^-	1.19	3.99	7.59	8.00

* previously published data [50].

It should be noted that the proton signals in the ^1H NMR spectra of the compounds **10–15** containing halide anions, and the proton signals of salts **16–21** containing NTf_2^- anions have identical multiplicity and exert very similar chemical shifts. This can be explained by the ability of compounds to form solvent-separated ion pairs. The quartet observed in the ^{13}C NMR spectra of compounds **16–21** at 120 ppm corresponds to the $\text{N}(\text{SO}_2\text{CF}_3)_2^-$ anion. The obtained salts **10–21** were characterized by ESI mass spectrometry. The mass spectra of the compounds **10–15** showed peaks corresponding to one-, two-, three-, and four-charged molecular ions without one, two, three, and four bromide anions. The obtained data also confirm the formation of solvate-separated ion pairs by the compounds **10–21**.

2.2. The Study of Thermal Stability of the Obtained Thiocalix[4]arene Based ILs

Melting point is one of the most important characteristics of ILs. Melting points of the synthesized thiocalix[4]arenes **10–21** are presented in Table 2. The replacement of halide ions by NTf_2^- ions leads to significant decrease of the melting points of the thiocalix[4]arenes by 39–55 °C. All synthesized macrocycles **16–21** containing NTf_2^- anions melt below 100 °C. It is well known that molecular packing density in the crystal lattice is a major factor affecting the melting point of the compound. More symmetrical molecules have denser packing in crystal and higher melting points. A comparison with the obtained results from previously published compounds with glycine residues [50] found that symmetrical *1,3-alternate* and *cone* stereoisomers showed higher melting points than asymmetrical *partial cone* structures. Thus, our hypothesis of lowering the melting point of *partial cone* stereoisomers (the compounds **12**, **13**, **18**, **19**) due to their molecular asymmetry was confirmed experimentally. However, the decrease of the melting point of the targeted compounds due to aromatic fragments in amino acid residues was not confirmed. The melting points of the macrocycles containing glycine fragments are lower by 1–11 °C compared to stereoisomers with *L*-phenylalanine fragments. Apparently, these results can be explained by the interaction of *L*-phenylalanine fragments with each other and the formation of additional hydrophobic and π - π interactions, which leads to a denser molecular packing in the crystal lattice and an increase in the melting point of the compounds as a result.

Table 2. Melting points (°C) of the macrocycles 10–21 containing amino acid fragments.

Amino Acid Fragments	Br [−]			N(SO ₂ CF ₃) ₂ [−]		
	Cone	Partial Cone	1,3-alternate	Cone	Partial Cone	1,3-alternate
Gly	114 * (10)	105 (12)	112 * (14)	63 * (16)	50 (18)	73 * (20)
L-Phe	118 (11)	110 (13)	123 (15)	64 (17)	55 (19)	75 (21)

* previously published data [50].

High thermal stability is one of the characteristic properties of ILs [52,53]. The correlation between the obtained macrocyclic ILs structure and their thermal stability (influence of macrocycle conformation and amino acid residues) was investigated via thermogravimetric analysis (TG). Figure 1 shows the TG curves for the compounds 16–21. All obtained macrocyclic ILs were thermally stable (decomposition temperature $T_{\text{onset}} = 305\text{--}327\text{ }^{\circ}\text{C}$). Glycine containing compounds decomposed at a higher temperature (by 3–19 °C) compared to the compounds containing *L*-phenylalanine fragments. Many low molecular weight compounds for biofuel technology are obtained by pyrolysis (thermal lysis) of oligo- and polypeptides at a temperature of 300–350 °C [54]. However, thermal decomposition of proteins occurs at temperatures between 175 and 250 °C. In our case, the decomposition temperature of the amino acids containing compounds 16–21 was significantly higher. The obtained results are also consistent with the literature data on the thermal stability of macrocyclic ILs [38,50]. Temperature data $T_{10\%}$ and $T_{50\%}$ corresponding to 10% and 50% weight loss on decomposition are presented in Table 3. These characteristics are important in materials thermal stability research. The difference between T_{onset} , $T_{10\%}$ and $T_{50\%}$ is the measure of decomposition rate [52,55]. T_{onset} and $T_{10\%}$ of the studied compounds differ by 0–3 °C. The difference between T_{onset} and $T_{50\%}$ is more considerable, namely 41–109 °C. These results correspond to decomposition rate of non-macrocyclic ILs containing quaternary ammonium fragments [56,57]. The differential scanning calorimetry (DSC) heating curves of the synthesized compounds (Figure S34) in the temperature range of 300–375 °C clearly show endo effects corresponding to the first stage of decomposition. The values of endo effects for the compounds 16, 18, 20 are similar (38–41 J/g) (Figure S34a). These values are larger for the compounds 17, 19, 21 (53–55 J/g) (Figure S34b). The further decomposition of the obtained compounds at temperatures above 375 °C is accompanied by exo effects.

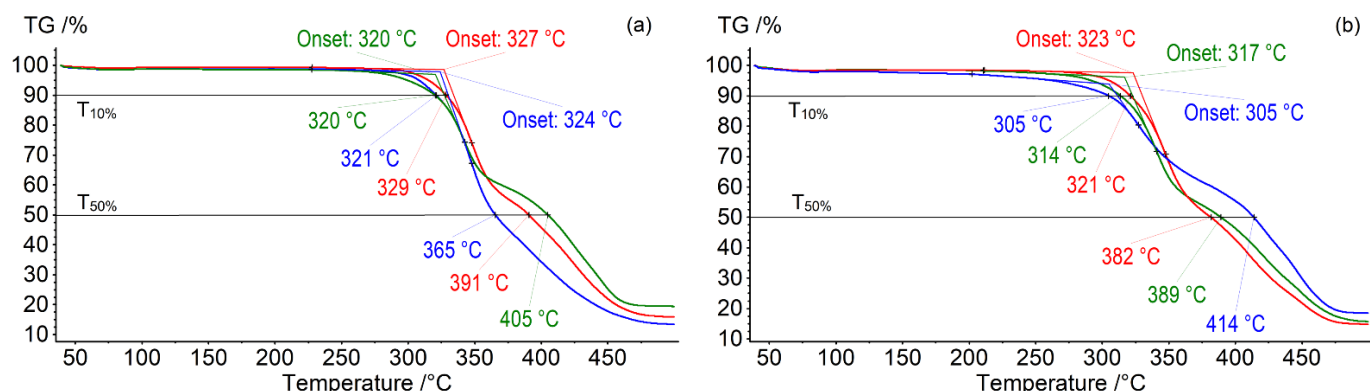
**Figure 1.** TG curves of the compounds with Gly: (a) 16 (green), 18 (blue), 20 (red), and *L*-Phe: (b) 17 (green), 19 (blue), 21 (red) fragments (dynamic argon atmosphere of 75 mL/min in the temperature range from 40 to 500 °C).

Table 3. TG data for the macrocyclic ILs 16–21 (°C).

Compounds	Amino Acid Fragments	T _{onset}	T _{10%}	T _{50%}
16 (cone)		320	320	405
18 (partial cone)	Gly	324	321	365
20 (1,3-alternate)		327	329	391
17 (cone)		317	314	389
19 (partial cone)	L-Phe	305	305	414
21 (1,3-alternate)		323	321	382

The experimental results and determined correlations between the synthesized macrocyclic ILs structure and their thermal characteristics showed that the introduction of aromatic amino acid (*L*-phenylalanine) fragments into ammonium salts based on *p*-*tert*-butylthiacalixarene reduces the thermal stability by 3–19 °C compared to glycine containing compounds. The melting points of the *L*-phenylalanine derivatives were higher than glycine ones by 1–11 °C. Oligo- and polypeptides thermal stability literature data [58–60] show that protein thermal stability increase is associated with rise of the number of charged amino acid fragments in their structures capable of electrostatic and cation– π interactions [61]. The presence of amino acids with uncharged polar fragments in protein structures reduces their thermal stability due to biomolecule packing efficiency decrease [62]. Thus, the obtained macrocyclic ILs are considered as biomimetic models of oligo- and polypeptides with the same structural patterns. The obtained results can also be applied to design of sensor systems capable for target substrate recognition.

3. Materials and Methods

3.1. General

All chemicals were purchased from Acros (Fair Lawn, NJ, USA), and most of them were used as received without additional purification. Organic solvents were purified by standard procedures. ¹H NMR and ¹³C NMR spectra were obtained on the Bruker Avance-400 spectrometer (Bruker Corp., Billerica, MA, USA) (¹³C{¹H} 100 MHz and ¹H 400 MHz). Chemical shifts were determined against the signals of residual protons of deuterated solvent (DMSO-*d*₆). The compounds concentration was equal to 3–5% by the weight in all records. The FTIR ATR spectra were recorded on the Spectrum 400 FT-IR spectrometer (Perkin–Elmer, Seer Green, Llantrisant, UK) with the Diamond KRS-5 attenuated total internal reflectance attachment (resolution 0.5 cm^{−1}, accumulation of 64 scans, recording time 16 s in the wavelength range 400–4000 cm^{−1}). Elemental analysis was performed on the Perkin–Elmer 2400 Series II instruments (Perkin–Elmer, Waltham, MA, USA). Melting points were determined using the Boetius Block apparatus (VEB Kombinat Nagema, Radebeul, Germany). Mass spectra (ESI) were recorded on an AmaZonX mass spectrometer (Bruker Daltonik GmbH, Bremen, Germany). The drying gas was nitrogen at 300 °C. The capillary voltage was 4.5 kV. The samples were dissolved in acetonitrile (concentration ~ 10^{−6} g mL^{−1}). ESI HRMS experiments were performed at Agilent 6550 iFunnel Q-TOF LC/MS (Agilent Technologies, Santa Clara, CA, USA), equipped with Agilent 1290 Infinity II LC. Simultaneous thermogravimetry (TG) and differential scanning calorimetry (DSC) of solid samples were performed using the thermoanalyzer STA 449F1 Jupiter (Netzsch, Germany) at the temperature range of 40–500 °C. The measurements were carried out in aluminum crucibles in a dynamic argon atmosphere (75 mL/min) at a temperature scanning rate of 10 °C/min. The weights of sample were 4.9–10.2 mg.

N-Bromoacetyl-glycine ethyl ester 5 and thiacalix[4]arenes 7–10, 14, 16, 20 were synthesized according to the literature procedures [50,63–65].

3.2. Procedure for the Synthesis of the Compound 4

L-Phenylalanine **2** (1 g, 6.05 mmol) was dissolved in 10 mL of ethanol in a round-bottom flask equipped with a magnetic stirrer. Thionyl chloride (0.88 mL, 12.10 mmol) was added dropwise with stirring. The reaction mixture was left for 30 min at room temperature, then the reaction was carried out under heating for 4 h. The solvent was removed on a rotary evaporator. Diethyl ether was added to the residue, after which the formed precipitate was filtered off. The obtained product was dried in vacuum over phosphorus pentoxide.

L-Phenylalanine Ethyl Ester Hydrochloride (**4**) [66]

^1H NMR (DMSO- d_6 , δ , ppm, J/Hz): 1.07 (t, $^3J_{\text{HH}} = 7.1$ Hz, 3H, $\text{CH}_3\text{CH}_2\text{O}$), 3.01–3.20 (m, 2H, CH_2Ph), 4.08 (m, 2H, $\text{CH}_3\text{CH}_2\text{O}$), 4.23 (m, 1H, NHCHCO), 7.22–7.35 (m, 5H, PhCH_2), 8.64 (br.s, 3H, NH_3^+).

3.3. Procedure for the Synthesis of the Compound 6

The solution of Na_2CO_3 (3.46 g, 32.66 mmol) in 50 mL of water was added to the suspension of L-phenylalanine ethyl ester hydrochloride **4** (3.41 g, 14.85 mmol) in benzene (50 mL). The reaction mixture was then cooled to 0 °C and bromoacetyl bromide (2.6 mL, 30 mmol) was added dropwise. The reaction mixture was allowed to warm to room temperature and stirred for 12 h with controlling pH = 6.5 by adding acetic acid. The organic phase was separated on a separating funnel and dried over anhydrous magnesium sulfate. Then the benzene was removed on a rotary evaporator. The obtained product **6** was dried in vacuum over phosphorus oxide.

N-Bromoacetyl-L-Phenylalanine Ethyl Ester (**6**) [66]

^1H NMR (DMSO- d_6 , δ , ppm, J/Hz): 1.11 (t, $^3J_{\text{HH}} = 7.1$ Hz, 3H, $\text{CH}_3\text{CH}_2\text{O}$), 2.90–3.05 (m, 2H, CH_2Ph), 3.86 (s, 2H, BrCH_2CO), 4.06 (q, $^3J_{\text{HH}} = 7.1$ Hz, 2H, $\text{CH}_3\text{CH}_2\text{O}$), 4.45 (m, 1H, NHCHCO), 7.20–7.30 (m, 5H, PhCH_2), 8.75 (d, $^3J_{\text{HH}} = 7.5$ Hz, 1H, CONHCH).

3.4. General Procedure for the Synthesis of the Compounds 10–15

The compounds **7–9** (0.30 g, 0.023 mmol) were dissolved in 5 mL of acetonitrile in a round-bottom flask equipped with a magnetic stirrer and reflux condenser. An equimolar amount per functional group (0.092 mmol) of the alkylating agent (N-bromoacetyl-glycine ethyl ester **5** or N-bromoacetyl-L-phenylalanine ethyl ester **6**) was added. The reaction mixture was refluxed for 18 h. Then the solvent was removed on a rotary evaporator. The obtained product was dried in vacuum over phosphorus oxide.

3.4.1. 5,11,17,23-Tetra-*tert*-butyl-25,26,27,28-tetrakis[N-[3'-(dimethyl){[(S)-ethoxycarbonylbenzylmethyl]aminocarbonylmethyl]ammonio}propyl]aminocarbonylmethoxy]-2,8,14,20-thiacalix[4]arene Tetrabromide in *cone* Conformation (**11**)

Yield: 0.57 g (96%). M.p. 118 °C. ^1H NMR (DMSO- d_6 , δ , ppm, J/Hz): 1.06 (s, 36H, $(\text{CH}_3)_3\text{C}$), 1.11 (t, $^3J_{\text{HH}} = 7.1$ Hz, 12H, $\text{CH}_3\text{CH}_2\text{O}$), 1.88 (m, 8H, $\text{NHCH}_2\text{CH}_2\text{CH}_2\text{N}^+$), 2.93 (m, 8H, CH_2Ph), 3.08 (s, 24H, $(\text{CH}_3)_2\text{N}^+$), 3.20 (m, 8H, $\text{NHCH}_2\text{CH}_2\text{CH}_2\text{N}^+$), 3.45 (m, 8H, $\text{NHCH}_2\text{CH}_2\text{CH}_2\text{N}^+$), 4.02–4.13 (m, 16H, $\text{CH}_3\text{CH}_2\text{O}$, $\text{N}^+\text{CH}_2\text{CO}$), 4.55 (m, 4H, NHCHCO), 4.80 (s, 8H, OCH_2CO), 7.21–7.30 (m, 20H, Ph), 7.38 (s, 8H, ArH), 8.51 (br.s, 4H, $\text{NHCH}_2\text{CH}_2\text{CH}_2\text{N}^+$), 9.12 (d, $^3J_{\text{HH}} = 7.5$ Hz, 4H, CONHCH). ^{13}C NMR (DMSO- d_6 , δ , ppm): 13.9, 22.6, 30.7, 33.9, 35.4, 36.5, 51.1, 53.7, 60.9, 61.7, 62.8, 74.2, 126.7, 128.1, 128.3, 129.1, 134.4, 136.6, 146.7, 157.9, 163.1, 168.3, 170.6. Elemental analysis. $\text{C}_{120}\text{H}_{168}\text{Br}_4\text{N}_{12}\text{O}_{20}\text{S}_4$ C, 56.60; H, 6.65; Br, 12.55; N, 6.60; S, 5.04. Found: C, 56.72; H, 6.85; Br, 12.23; N, 6.43; S, 4.79. MS (ESI), m/z : calculated for 556.5 $[\text{M}-4 \text{Br}^-]^{4+}$, 1192.5 $[\text{M}-2 \text{Br}^-]^{2+}$; found: 556.6 $[\text{M}-4 \text{Br}^-]^{4+}$, 1193.0 $[\text{M}-2 \text{Br}^-]^{2+}$. FTIR ATR (ν , cm^{-1}): 1095 (COC), 1677 (C=O), 3191 (N-H).

3.4.2. 5,11,17,23-Tetra-*tert*-butyl-25,26,27,28-tetrakis[*N*-[3'-(dimethyl[[ethoxycarbonylmethyl]aminocarbonylmethyl]ammonio)propyl]aminocarbonylmethoxy]-2,8,14,20-tetrathiacalix[4]arene Tetrabromide in *partial cone* Conformation (**12**)

Yield: 0.477 g (94%). M.p. 105 °C. ¹H NMR (DMSO-*d*₆, δ, ppm, *J*/Hz): 1.00 (s, 18H, (CH₃)₃C), 1.14–1.21 (m, 12H, CH₃CH₂O), 1.27 (s, 9H, (CH₃)₃C), 1.29 (s, 9H, (CH₃)₃C), 1.94 (m, 8H, NHCH₂CH₂CH₂N⁺), 3.13 (s, 6H, (CH₃)₂N⁺), 3.19 (s, 18H, (CH₃)₂N⁺), 3.39 (m, 8H, NHCH₂CH₂CH₂N⁺), 3.53 (m, 8H, NHCH₂CH₂CH₂N⁺), 3.93 (d, ³*J*_{HH} = 5.8 Hz, 8H, NHCH₂CO), 4.07–4.13 (m, 16H, CH₃CH₂O, N⁺CH₂CO), 4.40 (d, ²*J*_{HH} = 13.6 Hz, 2H, OCH₂C(O)), 4.49 (s, 2H, OCH₂C(O)), 4.51 (s, 2H, OCH₂C(O)), 4.80 (d, ²*J*_{HH} = 13.6 Hz, 2H, OCH₂C(O)), 7.01 (d, ⁴*J*_{HH} = 2.4 Hz, 2H, ArH), 7.65 (d, ⁴*J*_{HH} = 2.4 Hz, 2H, ArH), 7.67 (s, 2H, ArH), 7.75 (s, 2H, ArH), 8.32 (br.s, 2H, NHCH₂CH₂CH₂N⁺), 8.42 (br.s, 1H, NHCH₂CH₂CH₂N⁺), 8.50 (br.s, 1H, NHCH₂CH₂CH₂N⁺), 9.05. (m, 4H, CONHCH). ¹³C NMR (DMSO-*d*₆, δ, ppm): 14.1, 22.6, 30.7, 31.0, 33.8, 35.5, 40.8, 51.3, 60.8, 61.8, 62.7, 72.6, 126.4, 127.1, 127.6, 128.1, 133.7, 134.0, 135.1, 135.4, 145.3, 145.7, 146.5, 157.2, 159.4, 163.7, 166.9, 168.0, 168.8, 169.1. Elemental analysis. C₉₂H₁₄₄Br₄N₁₂O₂₀S₄ C, 50.55; H, 6.64; Br, 14.62; N, 7.69; S, 5.87; Found: C, 51.52; H, 6.25; Br, 14.26; N, 7.47; S, 5.89. HRMS (ESI), *m/z*: calculated for: 466.2370 [M–4 Br[–]]⁴⁺, 647.9557 [M–3 Br[–]]³⁺, 1012.3919 [M–2 Br[–]]²⁺; found: 466.2364 [M–4 Br[–]]⁴⁺, 647.9541 [M–3 Br[–]]³⁺, 1012.3937 [M–2 Br[–]]²⁺. FTIR ATR (ν, cm^{–1}): 1094 (COC), 1675 (C=O), 3207 (N–H).

3.4.3. 5,11,17,23-Tetra-*tert*-butyl-25,26,27,28-tetrakis[*N*-[3'-(dimethyl[(S)-ethoxycarbonylbenzylmethyl]aminocarbonylmethyl]ammonio)propyl]aminocarbonylmethoxy]-2,8,14,20-thiacalix[4]arene Tetrabromide in *partial cone* Conformation (**13**)

Yield: 0.551 g (93%). M.p. 110 °C. ¹H NMR (DMSO-*d*₆, δ, ppm, *J*/Hz): 1.00 (s, 18H, (CH₃)₃C), 1.10 (t, ³*J*_{HH} = 7.1 Hz, 12H, CH₃CH₂O), 1.27 (s, 9H, (CH₃)₃C), 1.28 (s, 9H, (CH₃)₃C), 1.85 (m, 8H, NHCH₂CH₂CH₂N⁺), 2.90–2.93 (m, 8H, CH₂Ph), 3.03 (s, 6H, (CH₃)₂N⁺), 3.09 (s, 18H, (CH₃)₂N⁺), 3.13–3.24 (m, 8H, NHCH₂CH₂CH₂N⁺), 3.46 (m, 8H, NHCH₂CH₂CH₂N⁺), 4.01–4.13 (m, 16H, CH₃CH₂O, N⁺CH₂CO), 4.42 (d, ²*J*_{HH} = 13.5 Hz, 2H, OCH₂C(O)), 4.48 (s, 2H, OCH₂C(O)), 4.51 (s, 2H, OCH₂C(O)), 4.55–4.60 (m, 4H, NHCHCO), 4.79 (d, ²*J*_{HH} = 13.5 Hz, 2H, OCH₂C(O)), 7.01 (d, ⁴*J*_{HH} = 2.4 Hz, 2H, ArH), 7.22–7.30 (m, 20H, Ph), 7.65 (d, 2H, ⁴*J*_{HH} = 2.4 Hz, ArH), 7.67 (s, 2H, ArH), 7.75 (s, 2H, ArH), 8.31 (br.s, 2H, NHCH₂CH₂CH₂N⁺), 8.41 (br.s, 1H, NHCH₂CH₂CH₂N⁺), 8.48 (br.s, 1H, NHCH₂CH₂CH₂N⁺), 9.12 (d, ³*J*_{HH} = 7.5 Hz, 4H, CONHCH). ¹³C NMR (DMSO-*d*₆, δ, ppm): 14.0, 22.6, 28.8, 30.7, 31.0, 33.8, 34.0, 35.5, 36.5, 51.2, 53.7, 54.0, 60.7, 61.0, 61.6, 61.8, 62.8, 63.1, 72.6, 126.4, 126.7, 127.1, 127.6, 128.3, 129.2, 133.7, 134.1, 135.1, 135.4, 136.6, 145.3, 145.7, 146.5, 157.2, 159.4, 163.2, 166.9, 168.0, 168.8, 170.7. Elemental analysis. C₁₂₀H₁₆₈Br₄N₁₂O₂₀S₄ C, 56.60; H, 6.65; Br, 12.55; N, 6.60; S, 5.04; found: C, 56.52; H, 6.55; Br, 12.26; N, 6.47; S, 4.89. HRMS (ESI), *m/z*: calculated for: 556.5348 [M–4 Br[–]]⁴⁺, 768.3527 [M–3 Br[–]]³⁺, 1192.4858 [M–2 Br[–]]²⁺; found: 556.5339 [M–4 Br[–]]⁴⁺, 768.3522 [M–3 Br[–]]³⁺, 1192.4872 [M–2 Br[–]]²⁺. FTIR ATR (ν, cm^{–1}): 1094 (COC), 1672 (C=O), 3187 (N–H).

3.4.4. 5,11,17,23-Tetra-*tert*-butyl-25,26,27,28-tetrakis[*N*-[3'-(dimethyl[(S)-ethoxycarbonylbenzylmethyl]aminocarbonylmethyl]ammonio)propyl]aminocarbonylmethoxy]-2,8,14,20-thiacalix[4]arene tetrabromide in *1,3-alternate* Conformation (**15**)

Yield: 0.574 g (97%). M.p. 123 °C. ¹H NMR (DMSO-*d*₆, δ, ppm, *J*/Hz): 1.12 (t, ³*J*_{HH} = 7.1 Hz, 12H, CH₃CH₂O), 1.19 (s, 36H, (CH₃)₃C), 1.90 (m, 8H, NHCH₂CH₂CH₂N⁺), 3.01 (m, 8H, CH₂Ph), 3.09 (s, 24H, (CH₃)₂N⁺), 3.15 (m, 8H, NHCH₂CH₂CH₂N⁺), 3.45 (m, 8H, NHCH₂CH₂CH₂N⁺), 4.00 (s, 8H, OCH₂CO), 4.01–4.14 (m, 16H, CH₃CH₂O, N⁺CH₂CO), 4.59 (m, 4H, NHCHCO), 7.20–7.30 (m, 20H, Ph), 7.59 (s, 8H, ArH), 8.02 (br.s, 4H, NHCH₂CH₂CH₂N⁺), 9.12 (d, ³*J*_{HH} = 7.6 Hz, 4H, CONHCH). ¹³C NMR (DMSO-*d*₆, δ, ppm): 13.9, 22.6, 30.7, 33.9, 35.4, 36.5, 51.1, 53.7, 60.9, 61.7, 62.8, 74.2, 126.7, 128.1, 128.3, 129.1, 134.5, 136.6, 146.7, 157.9, 163.1, 168.3, 170.6. Elemental analysis. C₁₂₀H₁₆₈Br₄N₁₂O₂₀S₄ C, 56.60; H, 6.65; Br, 12.55; N, 6.60; S, 5.04; found: C, 56.78; H, 6.26; Br, 12.21; N, 6.31; S, 4.07. MS (ESI), *m/z*: calculated: 556.5 [M–4 Br[–]]⁴⁺, 768.3 [M–3 Br[–]]³⁺, 1192.5 [M–2 Br[–]]²⁺, 2463.9 [M–Br[–]]⁺;

found: 556.5 [M-4 Br⁻]⁴⁺, 768.9 [M-3 Br⁻]³⁺, 1193.5 [M-2 Br⁻]²⁺, 2464.0 [M-Br⁻]⁺. FTIR ATR (ν , cm⁻¹): 1086 (COC), 1675 (C=O), 3186 (N-H).

3.5. General Procedure for the Synthesis of the Compounds 16–21

The compounds 10–15 (0.10 g) were dissolved in 2 mL of water in a round-bottom flask equipped with a magnetic stirrer and reflux condenser. An equimolar amount per functional group of the lithium bis(trifluoromethylsulfonyl)imide was added. The reaction mixture was stirred for 24 h. The resulting precipitate was filtered off. The obtained product was dried in vacuum over phosphorus oxide.

3.5.1. 5,11,17,23-Tetra-*tert*-butyl-25,26,27,28-tetrakis[N-(3'-(dimethyl[(S)-ethoxycarbonylbenzylmethyl]aminocarbonylmethyl)ammonio)propyl]aminocarbonylmethoxy}-2,8,14,20-thiacalix[4]arene tetra[bis(trifluoromethylsulfonyl)imide] in *cone* Conformation (17)

Yield: 0.127 g (97%). M.p. 64 °C. ¹H NMR (DMSO-*d*₆, δ , ppm, *J*/Hz): 1.06 (s, 36H, (CH₃)₃C), 1.12 (t, ³*J*_{HH} = 7.1 Hz, 12H, CH₃CH₂O), 1.86 (m, 8H, NHCH₂CH₂CH₂N⁺), 2.89–2.95 (m, 8H, CH₂Ph), 3.06 (s, 24H, (CH₃)₂N⁺), 3.20 (m, 8H, NHCH₂CH₂CH₂N⁺), 3.42 (m, 8H, NHCH₂CH₂CH₂N⁺), 3.98–4.09 (m, 16H, CH₃CH₂O, N⁺CH₂CO), 4.57 (m, 4H, NHCHCO), 4.79 (s, 8H, OCH₂CO), 7.19–7.29 (m, 20H, Ph), 7.38 (s, 8H, ArH), 8.48 (br.s, 4H, NHCH₂CH₂CH₂N⁺), 9.06 (d, ³*J*_{HH} = 7.5 Hz, 4H, CONHCH). ¹³C NMR (DMSO-*d*₆, δ , ppm): 13.9, 22.6, 30.7, 33.9, 35.4, 36.6, 51.2, 53.5, 61.0, 61.7, 62.6, 74.2, 119.5 (¹*J*_{CF} = 322 Hz), 126.8, 128.1, 128.4, 129.1, 134.5, 136.5, 146.8, 158.0, 163.1, 168.3, 170.6. Elemental analysis. C₁₂₈H₁₆₈F₂₄N₁₆O₃₆S₁₂ C, 45.93; H, 5.06; F, 13.62; N, 6.69; S, 11.49; found: C, 45.72; H, 5.85; F, 13.23; N, 6.43; S, 11.79. HRMS (ESI), *m/z*: calculated for: 556.5348 [M-4 NTf₂⁻]⁴⁺, 835.3524 [M-3 NTf₂⁻]³⁺; found: 556.5220 [M-4 NTf₂⁻]⁴⁺, 835.3328 [M-3 NTf₂⁻]³⁺. FTIR ATR (ν , cm⁻¹): 1094 (COC), 1668 (C=O), 3065 (N-H).

3.5.2. 5,11,17,23-Tetra-*tert*-butyl-25,26,27,28-tetrakis[N-(3'-(dimethyl[[ethoxycarbonylmethyl]aminocarbonylmethyl]ammonio)propyl]aminocarbonylmethoxy}-2,8,14,20-tetrathiacalix[4]arene tetra[bis(trifluoromethylsulfonyl)imide] in *partial cone* Conformation (18)

Yield: 0.131 g (96%). M.p. 50 °C. ¹H NMR (DMSO-*d*₆, δ , ppm, *J*/Hz): 1.00 (s, 18H, (CH₃)₃C), 1.14–1.20 (m, 12H, CH₃CH₂O), 1.27 (s, 9H, (CH₃)₃C), 1.30 (s, 9H, (CH₃)₃C), 1.93 (m, 8H, NHCH₂CH₂CH₂N⁺), 3.13 (s, 6H, (CH₃)₂N⁺), 3.18 (s, 18H, (CH₃)₂N⁺), 3.23–3.29 (m, 8H, NHCH₂CH₂CH₂N⁺), 3.52 (m, 8H, NHCH₂CH₂CH₂N⁺), 3.93 (d, ³*J*_{HH} = 5.8 Hz, 8H, OCH₂CH₃), 4.07 (m, 8H, N⁺CH₂CO), 4.13 (m, 8H, NHCH₂CO), 4.39 (d, ²*J*_{HH} = 13.6 Hz, 2H, OCH₂C(O)), 4.49 (s, 2H, OCH₂C(O)), 4.51 (s, 2H, OCH₂C(O)), 4.78 (d, ²*J*_{HH} = 13.6 Hz, 2H, OCH₂C(O)), 7.01 (d, ⁴*J*_{HH} = 2.4 Hz, 2H, ArH), 7.65 (d, ⁴*J*_{HH} = 2.4 Hz, 2H, ArH), 7.68 (s, 2H, ArH), 7.75 (s, 2H, ArH), 8.31 (br.s, 2H, NHCH₂CH₂CH₂N⁺), 8.41 (br.s, 1H, NHCH₂CH₂CH₂N⁺), 8.50 (br.s, 1H, NHCH₂CH₂CH₂N⁺), 9.05 (m, 4H, CONHCH). ¹³C NMR (DMSO-*d*₆, δ , ppm): 14.1, 22.6, 30.7, 31.0, 33.8, 35.5, 40.8, 51.3, 60.8, 61.8, 62.7, 72.6, 119.5 (¹*J*_{CF} = 322 Hz), 126.4, 127.1, 127.6, 128.1, 133.7, 134.0, 135.1, 135.4, 145.3, 145.7, 146.5, 157.2, 159.4, 163.7, 166.9, 168.0, 169.1. Elemental analysis. C₁₀₀H₁₄₄F₂₄N₁₆O₃₆S₁₂ C, 40.21; H, 4.86; F 15.26, N, 7.50; S, 12.88 found: C, 39.26; H, 4.46; F 15.08, N, 6.95; S, 12.49. HRMS (ESI), *m/z*: calculated for: 466.2370 [M-4 NTf₂⁻]⁴⁺, 715.2898 [M-3 NTf₂⁻]³⁺, 1212.8936 [M-2 NTf₂⁻]²⁺; found: 466.2357 [M-4 NTf₂⁻]⁴⁺, 715.2875 [M-3 NTf₂⁻]³⁺, 1212.8914 [M-2 NTf₂⁻]²⁺. FTIR ATR (ν , cm⁻¹): 1094 (C-O-C), 1674 (C=O), 3207 (N-H).

3.5.3. 5,11,17,23-Tetra-*tert*-butyl-25,26,27,28-tetrakis[N-(3'-(dimethyl[(S)-ethoxycarbonylbenzylmethyl]aminocarbonylmethyl)ammonio)propyl]aminocarbonylmethoxy}-2,8,14,20-thiacalix[4]arene tetra[bis(trifluoromethylsulfonyl)imide] in *partial cone* Conformation (19)

Yield: 0.125 g (95%). M.p. 55 °C. ¹H NMR (DMSO-*d*₆, δ , ppm, *J*/Hz): 1.00 (s, 18H, (CH₃)₃C), 1.10 (t, ³*J*_{HH} = 7.1 Hz, 12H, CH₃CH₂O), 1.27 (s, 9H, (CH₃)₃C), 1.28 (s, 9H, (CH₃)₃C), 1.86 (m, 8H, NHCH₂CH₂CH₂N⁺), 2.90–2.95 (m, 8H, CH₂Ph), 3.02 (s, 6H, (CH₃)₂N⁺), 3.08 (s, 18H, (CH₃)₂N⁺), 3.13–3.24 (m, 8H, NHCH₂CH₂CH₂N⁺), 3.42–3.45 (m,

8H, $\text{NHCH}_2\text{CH}_2\text{CH}_2\text{N}^+$), 4.04–4.07 (m, 16H, $\text{CH}_3\text{CH}_2\text{O}$, $\text{N}^+\text{CH}_2\text{CO}$), 4.40 (d, $^2J_{\text{HH}} = 13.5$ Hz, 2H, $\text{OCH}_2\text{C}(\text{O})$), 4.49 (s, 2H, $\text{OCH}_2\text{C}(\text{O})$), 4.52 (s, 2H, $\text{OCH}_2\text{C}(\text{O})$), 4.56–4.61 (m, 4H, NHCHCO), 4.79 (d, $^2J_{\text{HH}} = 13.5$ Hz, 2H, $\text{OCH}_2\text{C}(\text{O})$), 7.02 (d, $^4J_{\text{HH}} = 2.4$ Hz, 2H, ArH), 7.21–7.28 (m, 20H, Ph), 7.65 (d, $^4J_{\text{HH}} = 2.4$ Hz, 2H, ArH), 7.67 (s, 2H, ArH), 7.75 (s, 2H, ArH), 8.28 (br.s, 2H, $\text{NHCH}_2\text{CH}_2\text{CH}_2\text{N}^+$), 8.40 (br.s, 1H, $\text{NHCH}_2\text{CH}_2\text{CH}_2\text{N}^+$), 8.48 (br.s, 1H, $\text{NHCH}_2\text{CH}_2\text{CH}_2\text{N}^+$), 9.09. (m, 4H, CONHCH). ^{13}C NMR (DMSO- d_6 , δ , ppm): 13.9, 22.6, 30.7, 31.0, 33.8, 35.5, 36.6, 51.3, 53.6, 61.0, 61.7, 62.6, 72.6, 119.5 ($^1J_{\text{CF}} = 322$ Hz), 126.3, 126.8, 127.7, 128.4, 129.2, 133.7, 134.1, 135.2, 135.4, 136.6, 145.4, 145.7, 146.6, 157.3, 163.1, 168.0, 168.8, 170.7. Elemental analysis. $\text{C}_{128}\text{H}_{168}\text{F}_{24}\text{N}_{16}\text{O}_{36}\text{S}_{12}$ C, 45.93; H, 5.06; F, 13.62; N, 6.69; S, 11.49; found: C, 45.79; H, 5.00; F, 13.35; N, 6.43; S, 11.47. HRMS (ESI), m/z : calculated for: 556.5348 $[\text{M}-4 \text{NTf}_2^-]^{4+}$, 835.3524 $[\text{M}-3 \text{NTf}_2^-]^{3+}$; found: 556.5206 $[\text{M}-4 \text{NTf}_2^-]^{4+}$, 835.3283 $[\text{M}-3 \text{NTf}_2^-]^{3+}$. FTIR ATR (ν , cm^{-1}): 1096 (COC), 1668 (C=O), 3064 (N-H).

3.5.4. 5,11,17,23-Tetra-*tert*-butyl-25,26,27,28-tetrakis[N -[3'-(dimethyl{[(*S*)-ethoxycarbonylbenzylmethyl]aminocarbonylmethyl}ammonio)propyl]aminocarbonylmethoxy]-2,8,14,20-thiacalix [4]arene tetra[bis(trifluoromethylsulfonyl)imide] in 1,3-*alternate* Conformation (**21**)

Yield: 0.129 g (98%). M.p. 75 °C. ^1H NMR (DMSO- d_6 , δ , ppm, J/Hz): 1.12 (t, $^3J_{\text{HH}} = 7.1$ Hz, 12H, $\text{CH}_3\text{CH}_2\text{O}$), 1.19 (s, 36H, $(\text{CH}_3)_3\text{C}$), 1.89 (m, 8H, $\text{NHCH}_2\text{CH}_2\text{CH}_2\text{N}^+$), 2.91–2.96 (m, 8H, CH_2Ph), 3.08 (s, 24H, $(\text{CH}_3)_2\text{N}^+$), 3.15 (m, 8H, $\text{NHCH}_2\text{CH}_2\text{CH}_2\text{N}^+$), 3.43 (m, 8H, $\text{NHCH}_2\text{CH}_2\text{CH}_2\text{N}^+$), 3.99 (s, 8H, OCH_2CO), 4.03–4.07 (m, 16H, $\text{CH}_3\text{CH}_2\text{O}$, $\text{N}^+\text{CH}_2\text{CO}$), 4.59 (m, 4H, NHCHCO), 7.23–7.28 (m, 20H, Ph), 7.59 (s, 8H, ArH), 8.00 (br.s, 4H, $\text{NHCH}_2\text{CH}_2\text{CH}_2\text{N}^+$), 9.07 (d, $^3J_{\text{HH}} = 7.6$ Hz, 4H, CONHCH). ^{13}C NMR (DMSO- d_6 , δ , ppm): 13.9, 22.6, 30.8, 33.9, 35.8, 36.6, 51.2, 53.6, 61.0, 61.7, 62.5, 71.0, 119.5 ($^1J_{\text{CF}} = 322$ Hz), 126.7, 127.6, 128.4, 129.2, 133.1, 136.6, 146.1, 157.2, 163.1, 167.4, 170.7. Elemental analysis. $\text{C}_{128}\text{H}_{168}\text{F}_{24}\text{N}_{16}\text{O}_{36}\text{S}_{12}$ C, 45.93; H, 5.06; F, 13.62; N, 6.69; S, 11.49; found C, 45.22; H, 5.05; F, 13.53; N, 6.09; S, 11.09. HRMS (ESI), m/z : calculated for: 556.5348 $[\text{M}-4 \text{NTf}_2^-]^{4+}$, 835.3524 $[\text{M}-3 \text{NTf}_2^-]^{3+}$; found: 556.5198 $[\text{M}-4 \text{NTf}_2^-]^{4+}$, 835.3278 $[\text{M}-3 \text{NTf}_2^-]^{3+}$. FTIR ATR (ν , cm^{-1}): 1093 (COC), 1669 (C=O), 3064 (N-H).

4. Conclusions

Novel macrocyclic quaternary ammonium ILs containing amino acid fragments (glycine and *L*-phenylalanine) based on *p*-*tert*-butylthiacalix[4]arene in *cone*, *partial cone*, and 1,3-*alternate* conformations were synthesized. The melting temperature of the obtained ILs was found in the range of 50–75 °C. Replacement of the bromide anion with bis(trifluoromethylsulfonyl)imide led to a decrease in the melting point by 39–55 °C. The ILs in *partial cone* conformation had the lowest melting points among all stereoisomers. Thermal stability of the obtained macrocyclic ILs was determined via thermogravimetry and differential scanning calorimetry. The onset of decomposition of the synthesized compounds was established at 305–327 °C. The obtained results can be applied to the design of sensor systems capable for target substrate recognition. These compounds can also be used as synthetic biomimetic models of oligo- and polypeptides.

Supplementary Materials: The following are available online at <https://www.mdpi.com/article/10.3390/molecules27228006/s1>, Figures S1–S10: ^1H NMR spectra of the compounds **4**, **6**, **11–13**, **15**, **17–19**, **21**; Figures S11–S18: ^{13}C NMR spectra of the compounds **4**, **6**, **11–13**, **15**, **17–19**, **21**; Figures S19–S26: FT-IR spectra of the compounds **4**, **6**, **11–13**, **15**, **17–19**, **21**; Figures S27–S33: HRMS spectra of the compounds **4**, **6**, **11–13**, **15**, **17–19**, **21**; Figure S34: DSC curves of the compounds **16–21**.

Author Contributions: Conceptualization, writing—review and editing, supervision, I.S.; Project administration, writing—review and editing, funding acquisition and visualization, P.P.; writing—original draft preparation, investigation, O.T., A.B.; resources, formal analysis, A.G. All authors have read and agreed to the published version of the manuscript.

Funding: This work was financially supported by Russian Science Foundation, Russian Federation (grant № 19-73-10134, <https://rscf.ru/en/project/19-73-10134/>) (accessed on 1 November 2022).

Institutional Review Board Statement: Not applicable.

Informed Consent Statement: Not applicable.

Data Availability Statement: The data presented in this study are available in Supplementary Materials.

Acknowledgments: High resolution mass-spectrometry (ESI) has been carried out by the Kazan Federal University Strategic Academic Leadership Program ('PRIORITY-2030').

Conflicts of Interest: The authors declare no conflict of interest. The funders had no role in the design of the study; in the collection, analyses, or interpretation of data; in the writing of the manuscript, or in the decision to publish the results.

Sample Availability: Samples of all obtained compounds are available from the authors.

References

1. Patil, K.R.; Surwade, A.D.; Rajput, P.J.; Shaikh, V.R. Investigations of Solute–Solvent Interactions in Aqueous Solutions of Amino Acids Ionic Liquids Having the Common Nitrate as Anion at Different Temperatures. *J. Mol. Liq.* **2021**, *329*, 115546. [[CrossRef](#)]
2. Fabre, E.; Murshed, S.M.S. A Review of the Thermophysical Properties and Potential of Ionic Liquids for Thermal Applications. *J. Mater. Chem. A* **2021**, *9*, 15861–15879. [[CrossRef](#)]
3. Nikfarjam, N.; Ghomi, M.; Agarwal, T.; Hassanpour, M.; Sharifi, E.; Khorsandi, D.; Ali Khan, M.; Rossi, F.; Rossetti, A.; Nazarzadeh Zare, E.; et al. Antimicrobial Ionic Liquid-Based Materials for Biomedical Applications. *Adv. Funct. Mater.* **2021**, *31*, 2104148. [[CrossRef](#)]
4. Xu, C.; Yang, G.; Wu, D.; Yao, M.; Xing, C.; Zhang, J.; Zhang, H.; Li, F.; Feng, Y.; Qi, S.; et al. Roadmap on Ionic Liquid Electrolytes for Energy Storage Devices. *Chem. Asian J.* **2021**, *16*, 549–562. [[CrossRef](#)] [[PubMed](#)]
5. Minea, A.A.; Sohel Murshed, S.M. Ionic Liquids-Based Nanocolloids—A Review of Progress and Prospects in Convective Heat Transfer Applications. *Nanomaterials* **2021**, *11*, 1039. [[CrossRef](#)]
6. Buettner, C.S.; Cognigni, A.; Schröder, C.; Bica-Schröder, K. Surface-Active Ionic Liquids: A Review. *J. Mol. Liq.* **2022**, *347*, 118160. [[CrossRef](#)]
7. Correia, D.M.; Fernandes, L.C.; Fernandes, M.M.; Hermenegildo, B.; Meira, R.M.; Ribeiro, C.; Ribeiro, S.; Reguera, J.; Lanceros-Méndez, S. Ionic Liquid-Based Materials for Biomedical Applications. *Nanomaterials* **2021**, *11*, 2401. [[CrossRef](#)]
8. Maculewicz, J.; Świacka, K.; Stepnowski, P.; Dołzonek, J.; Białk-Bielińska, A. Ionic Liquids as Potentially Hazardous Pollutants: Evidences of Their Presence in the Environment and Recent Analytical Developments. *J. Hazard. Mater.* **2022**, *437*, 129353. [[CrossRef](#)]
9. Zhuang, W.; Hachem, K.; Bokov, D.; Javed Ansari, M.; Taghvaie Nakhjiri, A. Ionic Liquids in Pharmaceutical Industry: A Systematic Review on Applications and Future Perspectives. *J. Mol. Liq.* **2022**, *349*, 118145. [[CrossRef](#)]
10. Niu, H.; Wang, L.; Guan, P.; Zhang, N.; Yan, C.; Ding, M.; Guo, X.; Huang, T.; Hu, X. Recent Advances in Application of Ionic Liquids in Electrolyte of Lithium Ion Batteries. *J. Energy Storage* **2021**, *40*, 102659. [[CrossRef](#)]
11. Rauber, D.; Hofmann, A.; Philippi, F.; Kay, C.W.M.; Zinkevich, T.; Hanemann, T.; Hempelmann, R. Structure-Property Relation of Trimethyl Ammonium Ionic Liquids for Battery Applications. *Appl. Sci.* **2021**, *11*, 5679. [[CrossRef](#)]
12. Cho, C.-W.; Pham, T.P.T.; Zhao, Y.; Stolte, S.; Yun, Y.-S. Review of the Toxic Effects of Ionic Liquids. *Sci. Total Environ.* **2021**, *786*, 147309. [[CrossRef](#)] [[PubMed](#)]
13. El Seoud, O.A.; Keppeler, N.; Malek, N.I.; Galgano, P.D. Ionic Liquid-Based Surfactants: Recent Advances in Their Syntheses, Solution Properties, and Applications. *Polymers* **2021**, *13*, 1100. [[CrossRef](#)] [[PubMed](#)]
14. Gonçalves, A.R.P.; Paredes, X.; Cristino, A.F.; Santos, F.J.V.; Queirós, C.S.G.P. Ionic Liquids—A Review of Their Toxicity to Living Organisms. *Int. J. Mol. Sci.* **2021**, *22*, 5612. [[CrossRef](#)] [[PubMed](#)]
15. Himani; Pratap Singh Raman, A.; Babu Singh, M.; Jain, P.; Chaudhary, P.; Bahadur, I.; Lal, K.; Kumar, V.; Singh, P. An Update on Synthesis, Properties, Applications and Toxicity of the ILs. *J. Mol. Liq.* **2022**, *364*, 119989. [[CrossRef](#)]
16. Chen, Y.; Han, X.; Liu, Z.; Li, Y.; Sun, H.; Wang, H.; Wang, J. Thermal Decomposition and Volatility of Ionic Liquids: Factors, Evaluation and Strategies. *J. Mol. Liq.* **2022**, *366*, 120336. [[CrossRef](#)]
17. Holbrey, J.D.; Seddon, K.R. The Phase Behaviour of 1-Alkyl-3-Methylimidazolium Tetrafluoroborates; Ionic Liquids and Ionic Liquid Crystals. *J. Chem. Soc., Dalton Trans.* **1999**, *13*, 2133–2140. [[CrossRef](#)]
18. Shmukler, L.E.; Fedorova, I.V.; Fadeeva, Y.A.; Safonova, L.P. The Physicochemical Properties and Structure of Alkylammonium Protic Ionic Liquids of R_nH_{4-n}NX (n = 1–3) Family. A Mini-Review. *J. Mol. Liq.* **2021**, *321*, 114350. [[CrossRef](#)]
19. Vereshchagin, A.N.; Frolov, N.A.; Egorova, K.S.; Seitkalieva, M.M.; Ananikov, V.P. Quaternary Ammonium Compounds (QACs) and Ionic Liquids (ILs) as Biocides: From Simple Antiseptics to Tunable Antimicrobials. *Int. J. Mol. Sci.* **2021**, *22*, 6793. [[CrossRef](#)]
20. Zhuravlev, O.E.; Voronchikhina, L.L.; Gorbunova, D.V. Comparative Characteristics of Thermal Stability of Quaternary Ammonium and Pyridinium Tetrachloroferrates. *Russ. J. Gen. Chem.* **2022**, *92*, 348–354. [[CrossRef](#)]
21. Egorova, K.S.; Gordeev, E.G.; Ananikov, V.P. Biological Activity of Ionic Liquids and Their Application in Pharmaceutics and Medicine. *Chem. Rev.* **2017**, *117*, 7132–7189. [[CrossRef](#)] [[PubMed](#)]

22. Khachatryan, A.A.; Mukhametzyanov, T.A.; Yakhvarov, D.G.; Sinyashin, O.G.; Garifullin, B.F.; Rakipov, I.T.; Mironova, D.A.; Burilov, V.A.; Solomonov, B.N. Intermolecular Interactions between Imidazolium- and Cholinium-Based Ionic Liquids and Lysozyme: Regularities and Peculiarities. *J. Mol. Liq.* **2022**, *348*, 118426. [[CrossRef](#)]
23. Melo, C.I.; Bogel-Lukasik, R.; Nunes da Ponte, M.; Bogel-Lukasik, E. Ammonium Ionic Liquids as Green Solvents for Drugs. *Fluid Phase Equilib.* **2013**, *338*, 209–216. [[CrossRef](#)]
24. Bisht, M.; Jha, I.; Venkatesu, P. Comprehensive Evaluation of Biomolecular Interactions between Protein and Amino Acid Based-Ionic Liquids: A Comparable Study between [Bmim][Br] and [Bmim][Gly] Ionic Liquids. *ChemistrySelect* **2016**, *1*, 3510–3519. [[CrossRef](#)]
25. Schindl, A.; Hagen, M.L.; Muzammal, S.; Gunasekera, H.A.D.; Croft, A.K. Proteins in Ionic Liquids: Reactions, Applications, and Futures. *Front. Chem.* **2019**, *7*, 347. [[CrossRef](#)]
26. Ossowicz, P.; Klebko, J.; Roman, B.; Janus, E.; Rozwadowski, Z. The Relationship between the Structure and Properties of Amino Acid Ionic Liquids. *Molecules* **2019**, *24*, 3252. [[CrossRef](#)]
27. Miao, S.; Atkin, R.; Warr, G. Design and Applications of Biocompatible Choline Amino Acid Ionic Liquids. *Green Chem.* **2022**, *24*, 7281–7304. [[CrossRef](#)]
28. Shukla, S.K.; Mikkola, J.-P. Use of Ionic Liquids in Protein and DNA Chemistry. *Front. Chem.* **2020**, *8*, 598662. [[CrossRef](#)]
29. Egorova, K.S.; Posvyatenko, A.V.; Larin, S.S.; Ananikov, V.P. Ionic Liquids: Prospects for Nucleic Acid Handling and Delivery. *Nucleic Acids Res.* **2021**, *49*, 1201–1234. [[CrossRef](#)]
30. Patel, R.; Kumari, M.; Khan, A.B. Recent Advances in the Applications of Ionic Liquids in Protein Stability and Activity: A Review. *Appl. Biochem. Biotechnol.* **2014**, *172*, 3701–3720. [[CrossRef](#)]
31. Egorova, K.S.; Seitkalieva, M.M.; Posvyatenko, A.V.; Ananikov, V.P. An Unexpected Increase of Toxicity of Amino Acid-Containing Ionic Liquids. *Toxicol. Res.* **2015**, *4*, 152–159. [[CrossRef](#)]
32. Yadav, R.; Kahlon, N.K.; Kumar, S.; Devunuri, N.; Venkatesu, P. Biophysical Study on the Phase Transition Behaviour of Biocompatible Thermoresponsive Polymer Influenced by Tryptophan-Based Amino Acid Ionic Liquids. *Polymer* **2021**, *228*, 123871. [[CrossRef](#)]
33. Sahoo, D.K.; Jena, S.; Tulsiyan, K.D.; Dutta, J.; Chakrabarty, S.; Biswal, H.S. Amino-Acid-Based Ionic Liquids for the Improvement in Stability and Activity of Cytochrome c: A Combined Experimental and Molecular Dynamics Study. *J. Phys. Chem. B* **2019**, *123*, 10100–10109. [[CrossRef](#)]
34. Durga, G.; Kalra, P.; Kumar Verma, V.; Wangdi, K.; Mishra, A. Ionic Liquids: From a Solvent for Polymeric Reactions to the Monomers for Poly(Ionic Liquids). *J. Mol. Liq.* **2021**, *335*, 116540. [[CrossRef](#)]
35. Yang, B.; Yang, G.; Zhang, Y.-M.; Zhang, S.X.-A. Recent Advances in Poly(Ionic Liquid)s for Electrochromic Devices. *J. Mater. Chem. C* **2021**, *9*, 4730–4741. [[CrossRef](#)]
36. Barrulas, R.V.; Zannatta, M.; Casimiro, T.; Corvo, M.C. Advanced Porous Materials from Poly(Ionic Liquid)s: Challenges, Applications and Opportunities. *Chem. Eng. J.* **2021**, *411*, 128528. [[CrossRef](#)]
37. Thapaliya, B.P.; Puskar, N.G.; Slaymaker, S.; Feider, N.O.; Do-Thanh, C.-L.; Schott, J.A.; Jiang, D.; Teague, C.M.; Mahurin, S.M.; Dai, S. Synthesis and Characterization of Macrocyclic Ionic Liquids for CO₂ Separation. *Ind. Eng. Chem. Res.* **2021**, *60*, 8218–8226. [[CrossRef](#)]
38. Ogoshi, T.; Ueshima, N.; Yamagishi, T.; Toyota, Y.; Matsumi, N. Ionic Liquid Pillar[5]Arene: Its Ionic Conductivity and Solvent-Free Complexation with a Guest. *Chem. Commun.* **2012**, *48*, 3536. [[CrossRef](#)]
39. Zhou, J.; Rao, L.; Yu, G.; Cook, T.R.; Chen, X.; Huang, F. Supramolecular Cancer Nanotheranostics. *Chem. Soc. Rev.* **2021**, *50*, 2839–2891. [[CrossRef](#)]
40. Wang, M.; Fang, S.; Yang, S.; Li, Q.; Khashab, N.M.; Zhou, J.; Huang, F. Separation of Ethyltoluene Isomers by Nonporous Adaptive Crystals of Perethylated and Perbromoethylated Pillararenes. *Mater. Today Chem.* **2022**, *24*, 100919. [[CrossRef](#)]
41. Selivanova, N.; Gubaidullin, A.; Padnya, P.; Stoikov, I.; Galyametdinov, Y. Phase Behaviour, Structural Properties and Intermolecular Interactions of Systems Based on Substituted Thiacalix[4]Arene and Nonionic Surfactants. *Liq. Cryst.* **2018**, *46*, 415–421. [[CrossRef](#)]
42. Selivanova, N.M.; Zimina, M.V.; Padnya, P.L.; Stoikov, I.I.; Gubaidullin, A.T.; Galyametdinov, Y.G. Development of Efficient Luminescent Soft Media by Incorporation of a Hetero-Ligand Macrocyclic Terbium Complex into a Lyomesophase. *Russ. Chem. Bull.* **2020**, *69*, 1763–1770. [[CrossRef](#)]
43. Shurpik, D.N.; Padnya, P.L.; Stoikov, I.I.; Cragg, P.J. Antimicrobial Activity of Calixarenes and Related Macrocycles. *Molecules* **2020**, *25*, 5145. [[CrossRef](#)] [[PubMed](#)]
44. Yang, F.; Guo, H.; Jiao, Z.; Li, C.; Ye, J. Calixarene Ionic Liquids: Excellent Phase Transfer Catalysts for Nucleophilic Substitution Reaction in Water. *J. Iran. Chem. Soc.* **2012**, *9*, 327–332. [[CrossRef](#)]
45. Padnya, P.L.; Porfireva, A.V.; Evtugyn, G.A.; Stoikov, I.I. Solid Contact Potentiometric Sensors Based on a New Class of Ionic Liquids on Thiacalixarene Platform. *Front. Chem.* **2018**, *6*, 594. [[CrossRef](#)]
46. Padnya, P.L.; Terenteva, O.S.; Akhmedov, A.A.; Iksanova, A.G.; Shtyrlin, N.V.; Nikitina, E.V.; Krylova, E.S.; Shtyrlin, Y.G.; Stoikov, I.I. Thiacalixarene Based Quaternary Ammonium Salts as Promising Antibacterial Agents. *Bioorg. Med. Chem.* **2021**, *29*, 115905. [[CrossRef](#)]
47. Podyachev, S.N.; Zairov, R.R.; Mustafina, A.R. 1,3-Diketone Calix[4]Arene Derivatives—A New Type of Versatile Ligands for Metal Complexes and Nanoparticles. *Molecules* **2021**, *26*, 1214. [[CrossRef](#)]

48. Iampolska, A.D.; Kharchenko, S.G.; Voitenko, Z.V.; Shishkina, S.V.; Ryabitskii, A.B.; Kalchenko, V.I. Synthesis of Thiacalix[4]Arene Task-Specific Ionic Liquids. *Phosphorus Sulfur Silicon Relat. Elem.* **2016**, *191*, 174–179. [[CrossRef](#)]
49. Alishahi, N.; Mohammadpoor-Baltork, I.; Tangestaninejad, S.; Mirkhani, V.; Moghadam, M.; Kia, R. Calixarene Based Ionic Liquid as an Efficient and Reusable Catalyst for One-Pot Multicomponent Synthesis of Polysubstituted Pyridines and Bis-pyridines. *ChemistrySelect* **2019**, *4*, 5903–5910. [[CrossRef](#)]
50. Padnya, P.L.; Andreyko, E.A.; Gorbatova, P.A.; Parfenov, V.V.; Rizvanov, I.K.; Stoikov, I.I. Towards Macrocyclic Ionic Liquids: Novel Ammonium Salts Based on Tetrasubstituted *p*-Tert-Butylthiacalix[4]Arenes. *RSC Adv.* **2017**, *7*, 1671–1686. [[CrossRef](#)]
51. Zhang, S.; Sun, N.; He, X.; Lu, X.; Zhang, X. Physical Properties of Ionic Liquids: Database and Evaluation. *J. Phys. Chem. Ref. Data* **2006**, *35*, 1475–1517. [[CrossRef](#)]
52. Xu, C.; Cheng, Z. Thermal Stability of Ionic Liquids: Current Status and Prospects for Future Development. *Processes* **2021**, *9*, 337. [[CrossRef](#)]
53. Villanueva, M.; Coronas, A.; García, J.; Salgado, J. Thermal Stability of Ionic Liquids for Their Application as New Absorbents. *Ind. Eng. Chem. Res.* **2013**, *52*, 15718–15727. [[CrossRef](#)]
54. Moldoveanu, S.C. Pyrolysis of Amino Acids and Small Peptides. In *Pyrolysis of Organic Molecules*, 2nd ed.; Moldoveanu, S.C., Ed.; Elsevier: London, UK, 2019; pp. 555–633. [[CrossRef](#)]
55. Efimova, A.; Pfützner, L.; Schmidt, P. Thermal Stability and Decomposition Mechanism of 1-Ethyl-3-Methylimidazolium Halides. *Thermochim. Acta* **2015**, *604*, 129–136. [[CrossRef](#)]
56. Lorenzo, M.; Vilas, M.; Verdía, P.; Villanueva, M.; Salgado, J.; Tojo, E. Long-Term Thermal Stabilities of Ammonium Ionic Liquids Designed as Potential Absorbents of Ammonia. *RSC Adv.* **2015**, *5*, 41278–41284. [[CrossRef](#)]
57. Kurnia, K.A.; Wilfred, C.D.; Murugesan, T. Thermophysical Properties of Hydroxyl Ammonium Ionic Liquids. *J. Chem. Thermodyn.* **2009**, *41*, 517–521. [[CrossRef](#)]
58. Pucci, F.; Rooman, M. Improved Insights into Protein Thermal Stability: From the Molecular to the Structurome Scale. *Phil. Trans. R. Soc. A.* **2016**, *374*, 20160141. [[CrossRef](#)]
59. Wingreen, N.S.; Li, H.; Tang, C. Designability and Thermal Stability of Protein Structures. *Polymer* **2004**, *45*, 699–705. [[CrossRef](#)]
60. Maheshwari, A.S.; Archunan, G. Distribution of Amino Acids in Functional Sites of Proteins with High Melting Temperature. *Bioinformatics* **2012**, *8*, 1176–1181. [[CrossRef](#)]
61. Jelesarov, I.; Karshikoff, A. Defining the Role of Salt Bridges in Protein Stability. *Methods Mol. Biol.* **2008**, *490*, 227–260. [[CrossRef](#)]
62. Kumar, S.; Tsai, C.-J.; Nussinov, R. Factors Enhancing Protein Thermostability. *Protein Eng. Des. Sel.* **2000**, *13*, 179–191. [[CrossRef](#)] [[PubMed](#)]
63. Padnya, P.L.; Andreyko, E.A.; Mostovaya, O.A.; Rizvanov, I.K.; Stoikov, I.I. The Synthesis of New Amphiphilic *P*-Tert-Butylthiacalix[4]Arenes Containing Peptide Fragments and Their Interaction with DNA. *Org. Biomol. Chem.* **2015**, *13*, 5894–5904. [[CrossRef](#)] [[PubMed](#)]
64. Andreyko, E.A.; Padnya, P.L.; Stoikov, I.I. Supramolecular Self-Assembly of Water-Soluble Nanoparticles Based on Amphiphilic *p*-Tert-Butylthiacalix[4]Arenes with Silver Nitrate and Fluorescein. *Colloids Surf. A* **2014**, *454*, 74–83. [[CrossRef](#)]
65. Andreyko, E.A.; Padnya, P.L.; Daminova, R.R.; Stoikov, I.I. Supramolecular “Containers”: Self-Assembly and Functionalization of Thiacalix[4]Arenes for Recognition of Amino- and Dicarboxylic Acids. *RSC Adv.* **2014**, *4*, 3556–3565. [[CrossRef](#)]
66. Nazarova, A.; Shurpik, D.; Padnya, P.; Mukhametzyanov, T.; Cragg, P.; Stoikov, I. Self-Assembly of Supramolecular Architectures by the Effect of Amino Acid Residues of Quaternary Ammonium Pillar[5]Arenes. *Int. J. Mol. Sci.* **2020**, *21*, 7206. [[CrossRef](#)]